International Journal of Bifurcation and Chaos, Vol. 19, No. 8 (2009) 2755–2764
© World Scientific Publishing Company

AMPLITUDE EQUATION FOR STATIONARY CONVECTION IN A ROTATING BINARY FERROFLUID

D. LAROZE
Instituto de Alta Investigación, Universidad de Tarapacá, Casilla 7D, Arica, Chile

J. MARTINEZ-MARDONES
Instituto de Física, Pontificia Universidad Católica de Valparaíso, Casilla 4059, Valparaíso, Chile

L. M. PÉREZ
Departamento de Ingeniería Metalúrgica, Universidad de Santiago de Chile, Av. Bernardo OHiggins 3363, Santiago, Chile

Y. RAMESHWAR
Department of Mathematics, P. G. College of Science, Saifabad, Hyderabad 5000 04, India

Received April 19, 2008; Revised October 4, 2008

We report both theoretical and numerical results on convection for a binary magnetic mixture under rotation. We focus on the stationary convection for idealized boundary conditions. We obtain explicit expressions of convective thresholds in terms of the control parameters of the system. Close to bifurcation, the coefficients of the corresponding amplitude equation are determined analytically. The effect of the magnetophoresis and Kelvin force are emphasized and, finally, the nature of the bifurcation is discussed.

Keywords: Thermal convection; magnetic fluid; binary mixture.

1. Introduction

Ferrofluids are superparamagnetic fluids formed by a stable colloidal suspension of magnetic nanoparticles dispersed in a carrier liquid, and there are two main features that distinguish ferrofluids from ordinary fluids, the polarization force and the body couple. In the last decades, much efforts have been dedicated to the study of the phenomenon of convective mechanism in ferrofluids. In addition, heat transfer through magnetic fluids, in particular, have been one of the leading areas of scientific study due to its technological applications [Berkovsky *et al.*, 1973]. The ferrofluid convection has applications in high-power capacity transformer system where the ferrofluid is used as a material in the core as well as a coolant in the transform. To activate convective cooling, knowledge of concentration gradient, which will induce convection is required.

The first continuum description of the magnetic fluids was due to Neuringer and Rosensweig [1964]. Later, Finlayson [1970] studied the convective instability of a magnetic fluid for a fluid layer heated from below in the presence of a uniform vertical magnetic field. It discussed both shear free and rigid horizontal boundaries using the linear stability method. Convective instability for a

rotating layer of a magnetic fluid have been studied by Gupta and Gupta [1979], and Venkatasubramanian and Kaloni [1994]. Auernhammer and Brand [2000] formulated the Küppers–Lortz instability for a magnetic fluid. In addition, Ryskin and Pleiner [2004], using the nonequilibrium thermodynamics have derived a complete set of equations to describe ferrofluids in an external magnetic field. This description is made in terms of a binary mixture where the magnetophoretic effect, as well as magnetic stresses, have been taken into account in the static and dynamic parts of the ferrofluid equations. Recently, when the magnetophoretic effect have been neglected, we have analyzed the thermal convection for rotating ferrofluid for idealized boundary condition for the typical conductive state in the stationary case and it was found that an analytical expression for the Rayleigh number is a function of control parameters [Laroze *et al.*, 2006].

The purpose of this paper is to analyze the influence of magnetophoretic effect and the coupling between the concentration and magnetic effect in the rotating convective thresholds of the binary magnetic mixtures for idealized boundary conditions. To this aim, a binary mixture of ferrofluids heated from below and rotated around the vertical axis is considered. A linear stability analysis of the conduction state is performed in the framework of Navier–Stokes equations and we have obtained explicit expressions of convective thresholds in terms of the control parameters of the system. The weakly nonlinear analysis for stationary convection is performed and the explicit coefficients of the amplitude equation are calculated. For a critical value of the parameters, the coefficient of the cubic nonlinearity of the amplitude equation is zero, then the system exhibits a transition between supercritical and subcritical bifurcation. The paper is organized as follows: In Sec. 2, the basic hydrodynamic equations for binary magnetic mixture convection are presented. In Sec. 3 the linear stability analysis of the conduction state is performed, in the case of idealized boundary condition, and we find an analytical expression of the Rayleigh number. In Sec. 4, the weakly nonlinear analysis is developed and we find the explicit expression for the coefficient of the stationary amplitude equation; also we show that due to rotational effects a supercritical–subcritical transition appears. In Sec. 5 the wavelength instabilities are discussed. Finally, conclusions are presented in Sec. 6.

2. Theoretical Model

We consider a layer of incompressible binary magnetic fluid, of thickness d, parallel to the xy-plane, with very large horizontal extension, in a gravitational field $\mathbf{g}$ and submitted to a vertical temperature gradient. The layer is rotating uniformly about the vertical with uniform angular velocity $\boldsymbol{\varpi}$. The magnetic fluid properties can be modeled as electrically nonconducting superparamagnets, and it is assumed to be placed in a magnetic field $\mathbf{H}$ parallel to $\hat{\mathbf{z}}$, which would be homogeneous if the magnetic fluid were absent. Let us choose the z-axis such that $\mathbf{g} = -g\hat{\mathbf{z}}$ and that the layer has its interfaces at $z = -d/2$ and $z = d/2$ (see Fig. 1). Under the Boussinesq approximation, the dimensionless balance equations of the conduction read as

$$\nabla \cdot \mathbf{v} = 0, \tag{1}$$

$$\rho_0 D_t \mathbf{v} = -\nabla p_{\text{eff}} + \nu \nabla^2 \mathbf{v} + \rho \mathbf{g} + 2\rho_0 \boldsymbol{\varpi} \times \mathbf{v} + \mathbf{M} \cdot \nabla \mathbf{H}, \tag{2}$$

$$\frac{c_{v,\mathbf{H}}}{T_0} D_t T + \chi_T \mathbf{H}_0 \cdot D_t \mathbf{H} = \bar{\kappa} \nabla^2 T + \frac{D_f c_{v,\mathbf{H}}}{T_0} \nabla^2 C + D_s \chi_c \mathbf{H}_0 \cdot \nabla^2 \mathbf{H}, \tag{3}$$

$$D_t C = D_c \nabla^2 C + D_s \nabla^2 T + \frac{D_c \chi_c}{\gamma_H} \mathbf{H}_0 \cdot \nabla^2 \mathbf{H}, \tag{4}$$

with

$$p_{\text{eff}} = p_0 + \frac{H^2 + \rho_0 |\varpi \times \mathbf{r}|}{2},$$

where $D_t f = \partial_t f + \mathbf{v} \cdot \nabla f$ is the material derivative and $\mathbf{v}$ the velocity field, p_{eff} the effective pressure, ρ the mass density, ρ_0 a reference mass density, ν the viscosity, $\mathbf{M}$ the magnetization field, $c_{v,\mathbf{H}}$ the specific heat capacity at constant volume and magnetic

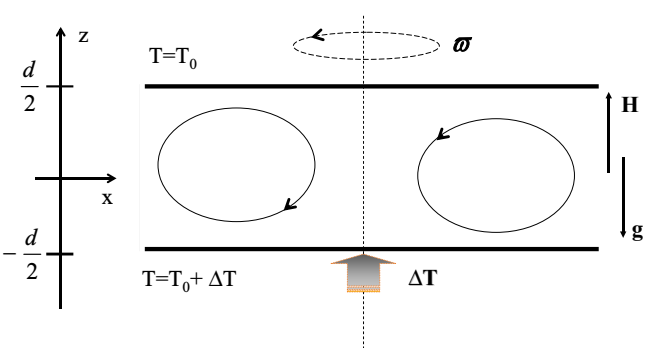


Fig. 1. A vertical cut through the fluid layer. Note the y-axis point in the xz-plane.

field, T the temperature, T_0 a reference temperature, χ_T the pyromagnetic coefficient, $\overline{\kappa}$ the thermal diffusivity, C the magnetic particle concentration, D_s the Soret coefficient, D_c the diffusion coefficient and D_f the Dufour coefficient.

For the total density we use the following linear state equation

$$\rho = \rho_0(1 - \alpha_T \triangle T + \alpha_c \triangle C + \alpha_H \mathbf{H}_0 \cdot \triangle \mathbf{H}) \quad (5)$$

where α_T, α_c and α_c are the thermal, the mass and the magnetic expansion coefficients, respectively; and $\triangle f = f - f_0$. In addition, for the magnetic field $\mathbf{H}$ and the magnetic induction $\mathbf{B}$, we suppose that the system is not a conductor, that is, it is governed by the Maxwell equation:

$$\nabla \times \mathbf{H} = \mathbf{0}, \quad (6)$$

$$\nabla \cdot \mathbf{B} = 0. \quad (7)$$

Furthermore the relationship between these fields $\mathbf{B} = \mathbf{H} + \mathbf{M}$ and note that from Eq. (6) the magnetic field can be of the form of the scalar magnetic potential $\mathbf{H} = -\nabla\phi$. For the magnetization field we use the typical phenomenological state equation $\mathbf{M} = \hat{\mathbf{H}} M(T, C, H)$:

$$M(T, C, H) = M_0 - \chi_T \triangle T + \chi_c \triangle C + \chi_H \mathbf{H}_0 \cdot \triangle \mathbf{H} \quad (8)$$

Now we analyzed the boundary conditions (BCs); thermal BCs, a static temperature difference across the layer is imposed, $T(z = -d/2) = T_0 + \triangle T$ and $T(z = d/2) = T_0$; for the BC concentration we impose the impermeable boundary conditions, hence $\mathbf{n}\cdot\nabla(C - (D_s/D_c)T + (\chi_c/\gamma_H)\mathbf{H}_0(\mathbf{n}\cdot\nabla)\mathbf{H}) = 0$ at both boundaries, where $\mathbf{n}$ is a unitary vector normal to the boundaries. Moreover, for the magnetic BCs we used the typical continuity condition $\mathbf{n} \times (\mathbf{H}_{\text{in}} - \mathbf{H}_{\text{ex}}) = \mathbf{0}$ and $\mathbf{n} \cdot (\mathbf{B}_{\text{in}} - \mathbf{B}_{\text{ex}}) = 0$. For velocity we will consider unrealistic free interfaces. Hence, from Eqs. (1)–(8) and using these boundary conditions the conductive basic state is

$$\mathbf{v}_{\text{con}} = \mathbf{0}, \quad (9)$$

$$T_{\text{con}}(z) = \overline{T} - \beta z, \quad (10)$$

$$C_{\text{con}}(z) = \overline{C}, \quad (11)$$

$$\mathbf{H}_{\text{con}}(z) = \mathbf{H}_0(1 + \lambda\beta z), \quad (12)$$

where $\beta = (\triangle T/d)$ and $\lambda = \chi_T/(1 + \chi_H)$. Therefore, the perturbation equation of the conducting state can be written as

$$\nabla \cdot \mathbf{v} = \mathbf{0} \quad (13)$$

$$(\partial_t + \mathbf{v} \cdot \nabla)(\theta - M_4\partial_z\phi) = (1 - M_4)w + \nabla^2\theta + F\nabla^2(c - M_2\partial_z\phi) \quad (14)$$

$$(\partial_t + \mathbf{v} \cdot \nabla)c = L\nabla^2(c + \theta - M_2\partial_z\phi) \quad (15)$$

$$P^{-1}(\partial_t + \mathbf{v} \cdot \nabla)\mathbf{v} = -\nabla p_{\text{eff}} + \nabla^2\mathbf{v} + R_a\Pi_1\hat{\mathbf{z}} + R_a\Pi_2\nabla(\partial_z\phi) + T_a^{1/2}\mathbf{v} \times \hat{\mathbf{z}} \quad (16)$$

$$(\partial_{zz} + M_3\nabla_\perp^2)\phi - \partial_z(\theta - \psi_m c) = 0 \quad (17)$$

$$\nabla^2\phi_{\text{ext}} = 0 \quad (18)$$

where $\Pi_1(\theta, c, \phi) = (1+M_1)\theta - (\psi + M_1\psi_m)c - (M_1 - M_5)\partial_z\phi$ and $\Pi_2(\theta, c) = M_1(\theta - \psi_m c)$. Also the following groups of dimensionless numbers have been introduced: (a) (pure fluids) the Rayleigh number $R_a = \alpha_T g \triangle T d^3/\kappa\nu$ accounting for buoyancy effects and the Prandtl number $P = \nu/\kappa$, relating viscous and thermal effects; (b) (binary mixtures) the Lewis number $L = D_c/\kappa$, relating diffusion with thermal diffusivity, the separation ratio $\psi = \alpha_c D_T/(\alpha_T D_c)$ and the Dufuor number $F = D_T^2/(D\kappa)$; (c) (magnetic fluid) the strength of magnetic force relative to buoyancy $M_1 = \beta\chi_T^2 H_0^2/(\rho_0 g \alpha_T(1 + \chi))$, the magnetophoretic number which gives rise to a field dependence of heat and concentration currents $M_2 = D\chi_c\chi_T H_0^2/(\rho_0 g\alpha_T(1 + \chi))$, the nonlinearity of magnetization $M_3 = 1 - (\chi_H H_0^2)/(1 + \chi)$ is a measure of the deviation of the magnetization curve from the linear behavior $M_0 = \chi_H H_0$, the relative strength of temperature dependence of the magnetic susceptibility $M_4 = \chi_T^2 H_0^2 T_0/c_0(1 + \chi)$, the ratio of magnetic to thermal buoyancy $M_5 = \alpha_H\chi_T H_0^2/(\alpha_T(1 + \chi))$ and the magnetic separation ratio $\psi_m = -\chi_c D_T/(\chi_T D_c)$; (d) (rotation in pure fluids) the Taylor number $T_a = (2\varpi d^2/\nu)^2$. Let us comment about the numerical values of the parameters; the parameters R_a and T_a may be changed in several orders of magnitude. The magnetic numbers have the following order of magnitude $M_1 = 10^{-4} - 10^1$, $M_3 \approx 1.1$, $M_4 \approx M_5 \approx 10^{-6}$ [Laroze *et al.*, 2006]. The values of M_4, M_5 and F are very small, so the following analysis will not take them into account.

Using the afore-mentioned assumptions, we can write Eqs. (13)–(17) in the following way:

$$\pounds\mathbf{u} + \mathbf{N}(\mathbf{u} \imath \mathbf{u}) = 0 \quad (19)$$

with $\mathbf{u} = (u, v, w, p, \theta, c, \phi)^T$ and where $\pounds$ is the spatio-temporal linear operator and $\mathbf{N}$ stands for the nonlinear part of the respective equations, and

they are given as:

$$\pounds = \begin{pmatrix} \frac{\partial}{\partial x} & \frac{\partial}{\partial y} & \frac{\partial}{\partial z} & 0 & 0 & 0 & 0 \\ \frac{1}{P}\frac{\partial}{\partial t} - \nabla^2 & -\sqrt{T_a} & 0 & \frac{\partial}{\partial x} & 0 & 0 & 0 \\ \sqrt{T_a} & \frac{1}{P}\frac{\partial}{\partial t} - \nabla^2 & 0 & \frac{\partial}{\partial y} & 0 & 0 & 0 \\ 0 & 0 & \frac{1}{P}\frac{\partial}{\partial t} - \nabla^2 & \frac{\partial}{\partial z} & -R_a(1+M_1) & R_a(\psi + \psi_m M_1) & R_a M_1 \frac{\partial}{\partial z} \\ 0 & 0 & -1 & 0 & \frac{\partial}{\partial t} - \nabla^2 & 0 & 0 \\ 0 & 0 & 0 & 0 & -\nabla^2 & \frac{1}{L}\frac{\partial}{\partial t} - \nabla^2 & M_2 \nabla^2 \frac{\partial}{\partial z} \\ 0 & 0 & 0 & 0 & -\frac{\partial}{\partial z} & \psi_m \frac{\partial}{\partial z} & \frac{\partial^2}{\partial z^2} + M_3 \nabla_\perp^2 \end{pmatrix} \tag{20}$$

and

$$\mathbf{N} = \begin{pmatrix} 0 \\ \frac{1}{P}\mathbf{v}\cdot\nabla u - R_a M_1 (\theta - \psi_m c)\frac{\partial^2 \phi}{\partial x \partial z} \\ \frac{1}{P}\mathbf{v}\cdot\nabla v - R_a M_1 (\theta - \psi_m c)\frac{\partial^2 \phi}{\partial y \partial z} \\ \frac{1}{P}\mathbf{v}\cdot\nabla w - R_a M_1 (\theta - \psi_m c)\frac{\partial^2 \phi}{\partial z^2} \\ \mathbf{v}\cdot\nabla\theta \\ \frac{1}{L}\mathbf{v}\cdot\nabla c \\ 0 \end{pmatrix} \tag{21}$$

In the next sections we will develop the linear and weakly nonlinear analysis.

3. Linear Stability Analysis

In order to calculate the linear stability analysis, we only need the linear parts of Eq. (19). The space-temporal dependencies of $\mathbf{u}(\mathbf{r}, t)$ are separated by the usual normal mode expansion:

$$\mathbf{u}(\mathbf{r}, t) = \mathbf{U}(z)\exp[i\mathbf{k}\cdot\mathbf{r}_\perp + st], \tag{22}$$

with $\mathbf{U} = (U, V, W, P, \Theta, \Psi, \Phi)^T$, where $\mathbf{k}$ is the horizontal wave number vector, $\mathbf{r}_\perp$ is the transversal vector and where $s = \sigma + i\Omega$ denotes the complex eigenvalues; σ is the growth factor of a perturbation, and Ω its frequency.

With the purpose to find analytical expressions we impose the following boundary conditions $U = V = W = 0$, $D^2U = D^2V = D^2W = 0$ and $\Theta = \Psi = D\Phi = 0$ in $z = \pm 1/2$; with $D^n f = \partial_z^n f$. For aqueous suspensions of ferrofluid, we can assume that the separation ratio $\psi > 0$, so as follow we will analyze only the stationary convection case [Ryskin & Pleiner, 2004]. Hence, the eigenvalue problem gives the Rayleigh number, and the stationary bifurcation is obtained for the condition of marginal linear stability $s = 0$. In the fundamental mode, we can introduce the ansatz on the z-component of velocity:

$$W(z) = \mathrm{Cos}[\pi z]. \tag{23}$$

Therefore, $\pounds\mathbf{u} = 0$ leads to

$$U(z) = -\frac{i\pi(k_x(k^2+\pi^2) + k_y\sqrt{T_a})}{k^2(k^2+\pi^2)}\sin[\pi z], \tag{24}$$

$$V(z) = -\frac{i\pi(k_y(k^2+\pi^2) - k_x\sqrt{T_a})}{k^2(k^2+\pi^2)}\sin[\pi z], \tag{25}$$

$$P(z) = \frac{\pi((k^2+\pi^2)^2 + T_a)}{k^2(k^2+\pi^2)}\sin[\pi z], \tag{26}$$

$$\Theta(z) = \frac{1}{k^2+\pi^2}\cos[\pi z], \tag{27}$$

$$\Psi(z) = \frac{-k^2 M_3 + (M_2 - 1)\pi^2}{(k^2+\pi^2)(k^2 M_3 + \pi^2(1 + M_2\psi_m))}\cos[\pi z], \tag{28}$$

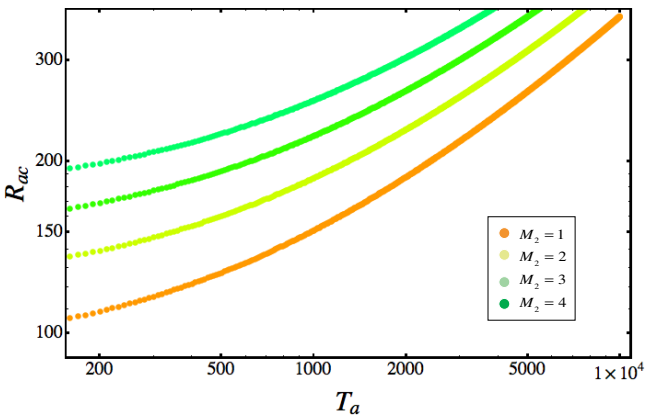


Fig. 2. Critical Rayleigh number R_{ac} as function of T_a for different values of M_2 at $M_1 = 10$, $M_3 = 1.1$ $\psi_m = 0.1$ and $\psi = 0.1$.

$$\Phi(z) = \frac{\pi(1+\psi_m)}{(k^2+\pi^2)(k^2M_3+\pi^2(1+M_2\psi_m))}\sin[\pi z]. \tag{29}$$

As solvability condition to the linear part of Eq. (19) we find the following relation of the parameters has a stationary instability (marginal curve)

$$R_a = \frac{(k^2M_3+\pi^2\Gamma)(\pi^2T_a+(\pi^2+k^2)^3)}{k^2[\pi^2(1+\psi+M_2(\psi_m-\psi))+k^2M_3\Lambda]} \tag{30}$$

where $\Gamma = 1 + M_2\psi_m$ and $\Lambda = 1 + \psi + M_1(1 + \psi_m)$. Note that, Eq. (30) reproduces all the known results, for instance, if we take $\psi = 0$, $\psi_m = 0$, $M_2 = 0$ we obtain the expression of R_a for a rotating magnetic fluid [Auernhammer & Brand, 2000]; and also, if we take $T_a = 0$ we recover R_a for a simple ferrofluid [Finlayson, 1970]. The minimum of the marginal curve ($\partial_k R_a = 0$) gives the critical wave number k_c and, the critical Rayleigh number, R_{ac}, can be obtained by replacing it in formula (30).

The main results are displayed in Fig. 2, where we plot the critical Rayleigh number, R_{ac}, as a function of the Taylor number, T_a, at $M_3 = 1.1$, $\psi = 1$ and $\psi_m = 1$ for different values of the magnetophoretic number M_2. We observe that, for these fixed parameters when M_2 increases, R_{ac} increases too. Also, we remark that, when M_1 and ψ_m increase the critical Rayleigh number decreases while it increases when the rotation ratio is increased. Therefore, binary effects are destabilized effects and the rotation stabilizes the system.

4. Weakly Nonlinear Analysis

In this section the evolution of the pattern is developed by means of a multiple scale analysis used by Newell, Whitehead and Segel [Newell & Whitehead, 1969; Segel, 1969]. We will assume that, a small amplitude convection cell is imposed on the basic flow. For values of the control parameter R_a given by Eq. (30) close to its threshold value R_{ac}, hence the bifurcation parameter will be

$$\epsilon^2 = \frac{R_a - R_{ac}}{R_{ac}} \tag{31}$$

We expand all functions in ϵ and assume that all variations of the linearized solutions can be incorporated into an amplitude function A. If this amplitude is of size of ϵ ($O(\epsilon)$) then the interaction of the cell with itself forces a second harmonic and a mean state of correction of size $O(\epsilon^2)$ and these in turn drive an $O(\epsilon^3)$ correction to the fundamental component of the imposed roll. A solvability criterion for this last correction yields an equation of the complex amplitude $A(X, Y, T)$ of the imposed disturbance, this is the Newell–Whitehead–Segel (NWS) equation. To simplify the problem we assume the formation of cylindrical rolls with axis parallel to y-axis so that y-dependence disappears from (19). The z-dependence is contained entirely in the sine and cosine functions, which ensures that the free-free boundary conditions are satisfied. Therefore, our expansion is

$$\mathbf{u} \to \epsilon A\{\mathbf{u}^{(0)} + \epsilon\mathbf{u}^{(1)} + \epsilon^2\mathbf{u}^{(2)} + \Theta(\epsilon^3)\} \tag{32}$$

Here $\mathbf{u}^{(0)}$ is the linear solution. Inserting the above equation into the governing Eq. (19), we expand there to obtain a hierarchy of equations

$$\epsilon^1 : \mathcal{L}^{(0)}\mathbf{u}^{(0)} = 0 \tag{33}$$

$$\epsilon^2 : \mathcal{L}^{(0)}\mathbf{u}^{(1)} = -N(\mathbf{u}^{(0)} \mid \mathbf{u}^{(0)}) \tag{34}$$

$$\epsilon^3 : \mathcal{L}^{(0)}\mathbf{u}^{(2)} = -\mathcal{L}^{(2)}\mathbf{u}^{(0)} - N(\mathbf{u}^{(0)} \mid \mathbf{u}^{(1)}) - N(\mathbf{u}^{(1)} \mid \mathbf{u}^{(0)}) \tag{35}$$

These equations must be solved iteratively each time fulfilling the solvability condition

$$\langle \mathbf{u}^\dagger \mid \text{r.h.s.} \rangle = \mathbf{0} \tag{36}$$

where $\mathbf{u}^\dagger$ are the solution of the kernel of the linear adjoint problem ($\mathcal{L}^+\mathbf{u}^\dagger = 0$). Also, r.h.s means the corresponding right-hand side of the perturbation equations and $\langle\circ\rangle$ denote the inner product which is an average over a suitable volume. The solvability condition at $O(\epsilon^3)$ leads to an equation

for amplitude A of type [Tagare *et al.*, 2008]:

$$\tau_0 \frac{\partial A}{\partial t} = \xi_0^2 \left(\frac{\partial}{\partial x} - \frac{i}{2k_c} \frac{\partial^2}{\partial y^2} \right)^2 A + \epsilon^2 A - g|A|^2 A \tag{37}$$

Equation (37) is the NWS equation and describes the variation of the slow time scale $\epsilon^2 t$ and slow spatial scales ϵx and $\sqrt{\epsilon} y$, perpendicular to the rolls. For $\epsilon = 0$, we do not get NWS. The coefficients of this equation can be calculated as [Auernhammer & Brand, 2000]:

$$\tau_0 = \left(R_{ac} \frac{\partial \sigma}{\partial R_a} \right)^{-1}_{R_{ac}} \tag{38}$$

$$\xi_0^2 = \frac{1}{2R_{ac}} \left(\frac{\partial^2 R_a}{\partial k^2} \right)_{R_{ac}} \tag{39}$$

$$g = \tau_0 \langle \mathbf{u}^\dagger \mid N(\mathbf{u}^{(0)} \mid \mathbf{u}^{(1)}) + N(\mathbf{u}^{(1)} \mid \mathbf{u}^{(0)}) \rangle_{R_{ac}} \tag{40}$$

The coefficients τ_0 and ξ_0^2 are known as growth rate amplitude and the curvature of the marginal stability curve, respectively. After straight-forward calculations, the explicit expressions of these coefficients can be written as

$$\tau_0 = \frac{(-1+P)\pi^2 T_a + (1+P) q_c^6}{P q_c^2 \Sigma} \tag{41}$$

$$\begin{aligned} \xi_0^2 = {} & \frac{4\Lambda^2 k_c^2 M_3^2}{(\pi^2 \Xi + \Lambda k_c^2 M_3)^2} + \frac{3k_c^4 M_3 q_c^2 (4k_c^2 + q_c^2)}{k_c^2 (\pi^2 \Gamma + k_c^2 M_3) \Sigma} \\ & + \frac{3\pi^2 \Gamma (\pi^2 T + 4k_c^4 q_c^2 - 3k_c^2 q_c^4 + q_c^6)}{k_c^2 (\pi^2 \Gamma + k_c^2 M_3) \Sigma} \\ & + \frac{\Lambda M_3 (3\pi^2 \Gamma (\pi^2 T - 4k_c^2 q_c^4 + q_c^6))}{(\pi^2 \Gamma + k_c^2 M_3)(\pi^2 \Xi + \Lambda k_c^2 M_3) \Sigma} \\ & - \frac{\Lambda M_3 (k_c^2 M_3 (\pi^2 T + 12 k_c^2 q_c^4 + q_c^6))}{(\pi^2 \Gamma + k_c^2 M_3)(\pi^2 \Xi + \Lambda k_c^2 M_3) \Sigma} \end{aligned} \tag{42}$$

$$\begin{aligned} g = {} & \frac{\pi^2 q_c^2 (k_c^2 (\Lambda + M_1) M_3 + \Xi \pi^2)}{2(\pi^2 \Gamma + (\Lambda - \psi) k_c^2 M_3)} \\ & - \frac{\pi^2 \Gamma q_c^2 T_a}{2P^2 k_c \Sigma} \end{aligned} \tag{43}$$

with $q^2 = k^2 + \pi^2$, $\Sigma = \pi^2 T_a + q_c^6$ and $\Xi = 1 + \psi + M_2(-\psi + \psi_m)$. Note that, we can recover some previous results, for instance, if we put $\psi = \psi_m = M_2 = 0$ we obtain

$$g_0 = \frac{\pi^2 q_c^2 (k_c^2 (1 + 2M_1) M_3 + \pi^2)}{2(\pi^2 + k_c^2 (1 + M_1) M_3)} - \frac{\pi^2 q_c^2 T_a}{2P^2 k_c \Sigma} \tag{44}$$

The last equation is the exactly cubic coefficient found by [Kaloni & Lou, 2004]. Figures 3 and 4 show the linear coefficients τ_0^{-1} and ξ_0^2 as a function of the Taylor number, T_a, at $M_1 = 10$, $M_2 = 1$ and $M_3 = 1.1$ for different values of separation ratio ψ and magnetic separation ratio ψ_M, respectively. From Fig. 3 we observe that τ_0 decreases both when T_a and ψ increase. Also, from Fig. 4 we observe that ξ_0^2 decreases when T_a increases, while it increases when ψ and ψ_M increase.

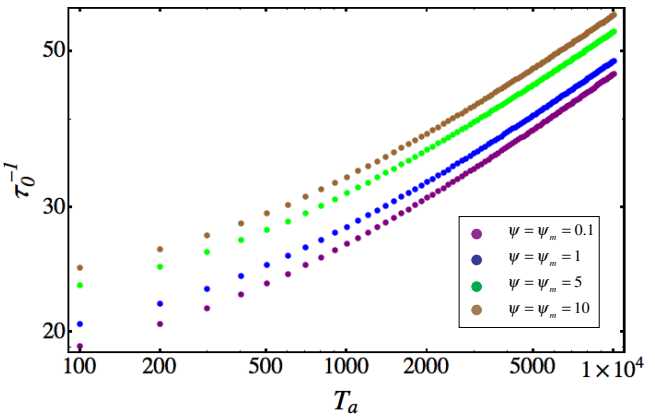


Fig. 3. τ_0^{-1} as a function of T_a for different values of the separation ratio ψ and the magnetic separation ratio ψ_m at $P = 10$, $M_1 = 10$, $M_2 = 1$ and $M_3 = 1.1$.

In addition, for $g > 0$ we get forward bifurcation (supercritical bifurcation), for $g < 0$ we get backward bifurcation (subcritical bifurcation), and at $g = 0$ we get tricritical bifurcation point which is the transition point between subcritical and supercritical bifurcations; and this critical transition is also denominated in supercritical quintic bifurcation. Figure 5 shows the normalized cubic nonlinear coefficient g as a function of T_a for different values of the separation ratio ψ and the magnetic separation

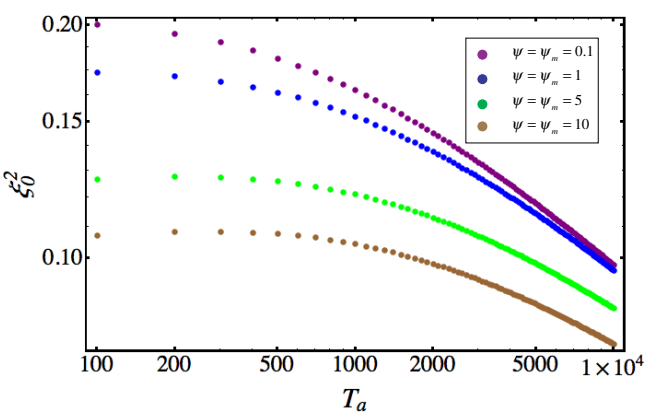


Fig. 4. ξ_0^2 as a function of T_a for different values of the separation ratio ψ and the magnetic separation ratio ψ_m at $P = 10$, $M_1 = 10$, $M_2 = 1$ and $M_3 = 1.1$.

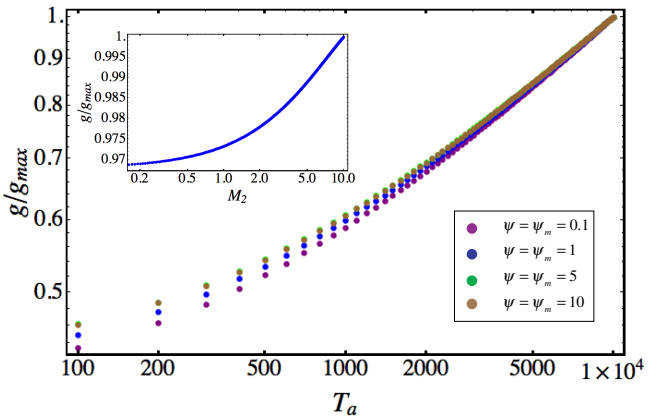


Fig. 5. Normalized cubic nonlinear coefficient $g/g_{\max}$ as a function of T_a for different values of the separation ratio ψ and the magnetic separation ratio ψ_m at $P = 10$, $M_1 = 10$, $M_2 = 1$ and $M_3 = 1.1$. The inset shows $g/g_{\max}$ as a function of M_2 at $M_1 = 10$, $M_3 = 1.1$, $\psi_m = 0.1$, $\psi = 0.1$ and $P = 10$ for $T_a = 0$ and $T_a = 10^3$.

ratio ψ_m at $M_1 = 10$, $M_2 = 1$ and $M_3 = 1.1$ and we observe that for low rotation rate when the binary effect increase the normalized nonlinear coefficient $g/g_{\max}$ increases too. In addition, we observe that g increases when M_2 increases, irrespective of the rotation rate (inset of Fig. 5). On the other hand, we numerically find that $g = 0$ and that $g < 0$ as is shown in Fig. 6 for some region of parameters; therefore a supercritical–subcritical transition appears. This phenomenon was observed before as a consequence of the rotational effect [Tagare *et al.*, 2008] (inset of Fig. 6). We remark that, our analysis is valid only for explaining the phenomenon when $g > 0$, but we have another range of physical parameters for $g < 0$ and in this case, it is necessary to use

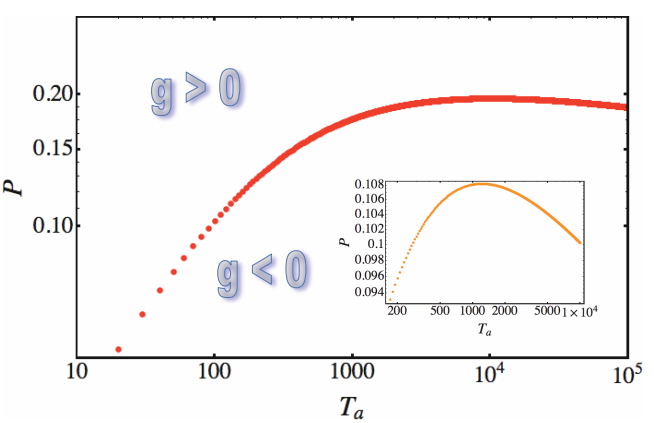


Fig. 6. Phase diagram of $P - T_a$ for the supercritical–subcritical transition at $M_1 = 10$, $M_2 = 10$, $M_3 = 1.1$, $\psi_m = 1$ and $\psi = 1$. The inset shows this diagram for a pure fluid.

the Cubic-Quintic Subcritical Newell–Whitehead-Segel equation [Clerc *et al.*, 2008], this model will be presented in future works.

Furthermore, for the stationary case dropping the y-dependences in Eq. (48), we have

$$\xi_0^2 \frac{\partial^2 A}{\partial x^2} + \epsilon^2 A - g\,|A|^2 A = 0 \tag{45}$$

and its analytical solution is

$$A(x) = A_0 \tanh(\zeta x) \tag{46}$$

where $A_0 = \sqrt{\epsilon^2/g}$ and $\zeta = \sqrt{\epsilon^2/2\xi_0^2}$. Hence, the maximum of steady amplitude A, denoted by $|A_{\max}|$, is given by $|A_{\max}| = \sqrt{\epsilon^2/g}$. We can use $A_{\max}$ to calculate Nusselt number, Nu. This number measures the ratio of the total heat transfer across a horizontal plane to the heat transfer by conduction alone, and it can be expressed as $\mathrm{Nu} = 1 + (\pi q_c)^2 |A_{\max}|^2/\sqrt{1+\epsilon}$; and from it, we get the convection for $\mathrm{Nu} > 1$ and conduction for $\mathrm{Nu} = 1$.

5. Wavelength Instabilities

To study the properties of stripe pattern with a given phase winding number $\delta k = k - k_c$ we substitute

$$A(x, y, t) = A_1(x, y, t)\exp(i\delta k_x) \tag{47}$$

into Eq. (37) and we obtain

$$\begin{aligned}\tau_0 \frac{\partial A_1}{\partial t} &= (\epsilon^2 - \xi_0^2 \delta k^2) A_1 \\ &\quad + 2i\xi_0^2 \delta k \left(\frac{\partial}{\partial x} - \frac{i}{2k_c}\frac{\partial^2}{\partial y^2}\right) A_1 \\ &\quad + \xi_0^2 \left(\frac{\partial}{\partial x} - \frac{i}{2k_c}\frac{\partial^2}{\partial y^2}\right)^2 A_1 - g|A_1|^2 A_1\end{aligned} \tag{48}$$

The steady state uniform solution of Eq. (48) is

$$A_1 = A_{1o} = \left[\frac{(\epsilon^2 - \xi_0^2 \delta k^2)}{g}\right]^{\frac{1}{2}} \tag{49}$$

Let $\tilde{u}(x, y, t) + i\tilde{v}(x, y, t)$ be an infinitesimal perturbation from a uniform steady state solution A_{1o} given by Eq. (49). Now substituting

$$A_1 = \left[\frac{(\epsilon^2 - \xi_0^2 \delta k^2)}{g}\right]^{\frac{1}{2}} + \tilde{u} + i\tilde{v} \tag{50}$$

into Eq. (48) and equating real and imaginary parts, we obtain

$$\tau_0\frac{\partial\tilde{u}}{\partial t}=\left[-2(\epsilon^2-\xi_0^2\delta k^2)+\xi_0^2\frac{\partial^2}{\partial x^2}+\frac{\xi_0^2\delta k}{k_c}\frac{\partial^2}{\partial y^2}-\frac{\xi_0^2}{4k_c^2}\frac{\partial^4}{\partial y^4}\right]\tilde{u}-\left(2\xi_0^2\delta k-\frac{\xi_0^2}{k_c}\frac{\partial^2}{\partial y^2}\right)\frac{\partial\tilde{v}}{\partial x} \tag{51}$$

$$\tau_0\frac{\partial\tilde{v}}{\partial t}=\left(2\xi_0^2\delta k-\frac{\xi_0^2}{k_c}\frac{\partial^2}{\partial y^2}\right)\frac{\partial\tilde{u}}{\partial x}+\xi_0^2\left(\frac{\partial^2}{\partial x^2}+\frac{\delta k}{k_c}\frac{\partial^2}{\partial y^2}-\frac{1}{4k_c^2}\frac{\partial^4}{\partial y^4}\right)\tilde{v} \tag{52}$$

We analyze Eqs. (51) and (52) by using normal modes of the form

$$\tilde{u}=U\exp[St]\cos(k_x x)\cos(k_y y) \tag{53}$$

$$\tilde{v}=V\exp[St]\sin(k_y x)\cos(k_y y) \tag{54}$$

Putting these normal modes into Eqs. (51) and (52) we get,

$$\left[\tau_0 S+2(\epsilon^2-\xi_0^2\delta k^2)+\xi_0^2k_x^2+\frac{\xi_0^2\delta k}{k_c}k_y^2+\frac{\xi_0^2}{4k_c^2}k_y^4\right]U+\left(2\delta k+\frac{k_y^2}{q_c}\right)\xi_0^2k_xV=0, \tag{55}$$

$$\xi_0^2k_x\left(2\delta k+\frac{k_y^2}{q_c}\right)U+\left(\tau_0S+\xi_0^2k_x^2+\frac{\xi_0^2\delta k}{k_c}k_y^2+\frac{\xi_0^2}{4k_c^2}k_y^4\right)V=0 \tag{56}$$

On solving Eqs. (55) and (56), it is possible to find the dispersion relationship:

$$\tau_0^2S^2+2S\left[2\tau_0(\epsilon^2-\xi_0^2\delta k^2)+\tau_0\xi_0^2k_x^2+\frac{\tau_0\xi_0^2}{k_c}k_y^2\delta k+\frac{\tau_0\xi_0^2}{4k_c^2}k_y^4\right]+\left[2(\epsilon^2-\xi_0^2\delta k^2)+\xi_0^2k_x^2+\frac{\xi_0^2}{k_c}k_y^2\delta k+\frac{\xi_0^2}{4k_c^2}k_y^4\right]\times\left[\xi_0^2k_x^2+\frac{\xi_0^2\delta k}{k_c}k_y^2+\frac{\xi_0^2}{4k_c^2}k_y^4\right]-k_x^2\xi_0^4\varsigma^2=0 \tag{57}$$

where $\varsigma=2\delta k+k_y^2/k_c$. The above equation is a quadratic equation on S, so it will be two real roots, $(S\pm)$ and are then defined as

$$S(\pm)=-\frac{1}{\tau_0^2}[2\tau_0(\epsilon^2-\xi_0^2\delta k^2)]-\frac{1}{\tau_0^2}\left[\tau_0\xi_0^2k_x^2+\frac{\tau_0\xi_0^2}{k_c}k_y^2\delta k+\frac{\tau_0\xi_0^2}{4{k_c}^2}k_y^4\right]\mp\frac{1}{\tau_0^2}\left[(2\tau_0(\epsilon^2-\xi_0^2\delta k^2))^2+\xi_0^2k_x^2\left(2\delta k+\frac{k_y^2}{k_c}\right)^2\right]^{\frac{1}{2}} \tag{58}$$

We note that, solution $S(-)$ is clearly negative, thus the corresponding mode is stable and if $S(+)$ is positive then rolls can be unstable. Symmetry considerations help us to restrict the study $S(+)$ to a domain $(k_x\geq 0, k_y\geq 0)$. In this next subsections we study two important instabilities.

5.1. *Longitudinal perturbations and Eckhaus instability*

Inserting $k_y=0$ into Eq. (58), we get

$$\tau_0^2+2S(2\tau_0(\epsilon^2-\xi_0^2\delta k^2)+\tau_0\xi_0^2k_x^2)+\xi_0^2k_x^2[2(\epsilon^2-3\xi_0^2\delta k^2)+k_x^2]=0. \tag{59}$$

Since the roots are real and their sum is always negative, the pattern is stable as long as both roots are negative, i.e. their product is positive. The stripe pattern becomes unstable when the product is negative, i.e. when $k_x^2\geq 2(\delta k^2-1/\xi_0^2)$ and $k_x^2\leq 2(3\xi_0^2\delta k^2-\epsilon^2)$ for this requires $\sqrt{\epsilon^2/3\xi_0^2}\leq|\delta k|\leq\sqrt{\epsilon^2/\xi_0^2}$; this condition defines the domain of the Eckhaus instability. The above condition implies that the most unstable wave vector tends to zero, when $|\delta k|\to\sqrt{\epsilon^2/3\xi_0^2}$.

5.2. *Transverse perturbations and zigzag instability*

Let us consider Eq. (58), we get

$$\tau_0^2S^2+2S\left[2\tau_0(\epsilon^2-\xi_0^2\delta k^2)+\frac{\tau_0\xi_0^2}{k_c}k_y^2\delta k+\frac{\tau_0\xi_0^2}{4k_c^2}k_y^4\right]+\left[2(\epsilon^2-\xi_0^2\delta k^2)+\frac{\xi_0^2}{k_c}k_y^2\delta k+\frac{\xi_0^2}{4k_c^2}k_y^4\right]\times\left[\frac{\delta k}{k_c}+\frac{k_y^2}{4k_c^2}\right]\xi_0^2k_y^2=0. \tag{60}$$

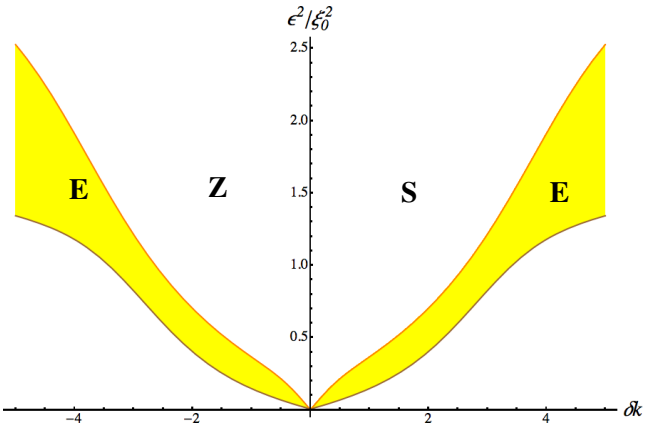


Fig. 7. Regions of Eckhuas instability (E), zigzag instability (Z) and stable region (S) are plotted at $\psi = 0.1$, $\psi_m = 0.1$, $M_1 = 10$, $M_2 = 1$, $M_3 = 1.1$ and $T_a = 10^3$.

The two eigen modes are uncoupled and we have $S(-)$,

$$S(-) = -2(\epsilon^2 - \xi_0^2 \delta k^2) - \frac{\xi_0^2}{k_c} k_y^2 \delta k - \frac{\xi_0^2}{4k_c^2} k_y^4 < 0 \tag{61}$$

for one of them. The other is amplified when

$$S(+) = -\xi_0^2 \, k_y^2 \left(\delta k + \frac{k_y^2}{4k_c} \right) > 0. \tag{62}$$

This implies that $\delta k < 0$ defines the domain of the zigzag instability. Since $\xi_0^2 > 0$, we get $|\delta k| > k_y^2/4k_c$.

Figures 7 and 8 show the Regions of Eckhuas instability and zigzag instability. We observe that when the magnetophoretic effect increases these regions change drastically. In addition, the effect of rotation rate on long wavelength instabilities is

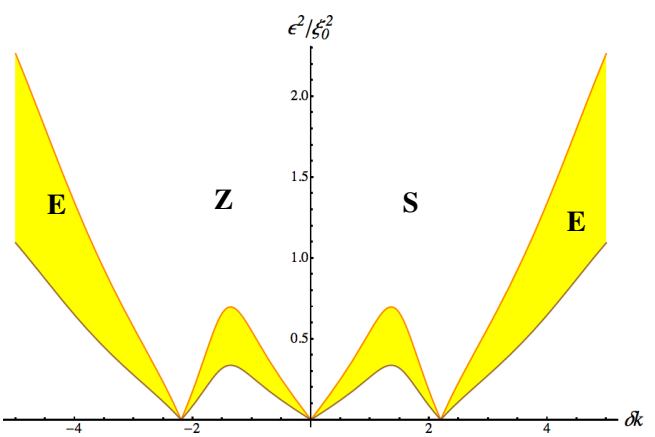
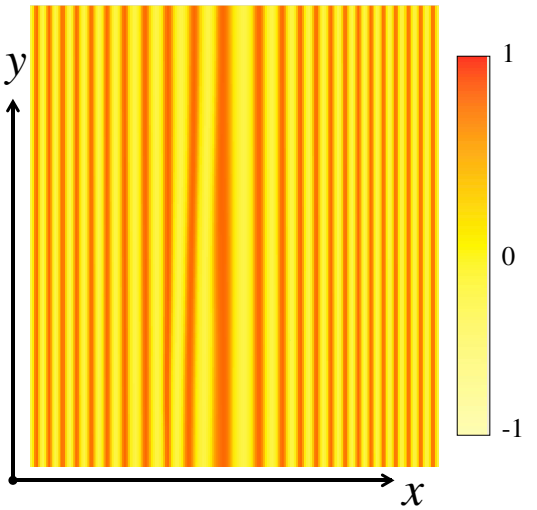
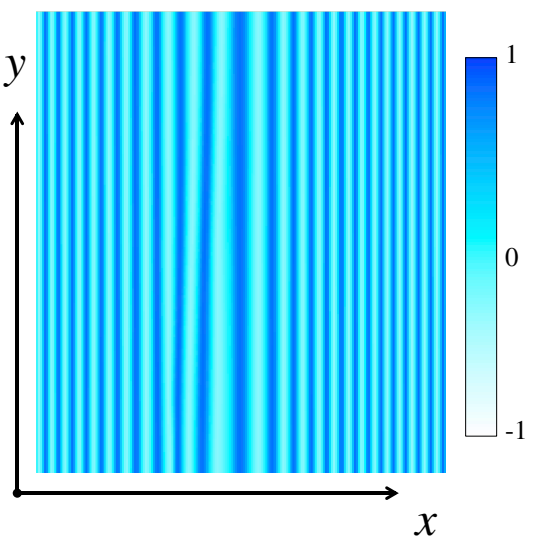


Fig. 8. Regions of Eckhuas instability (E), zigzag instability (Z) and stable region (S) are plotted at $\psi = 0.1$, $\psi_m = 0.1$, $M_1 = 10$, $M_2 = 10$, $M_3 = 1.1$ and $T_a = 10^3$.



(a)



(b)

Fig. 9. 2D diagrams for the real and the imaginary parts of amplitude Eq. (37) at $k_c = 5$ and $\epsilon = 0.3$.

observed, the Eckhuas instability and zigzag instability regions increase when T_a increases. Figure 9 shows 2D simulations of **Re**$[A]$ and **Im**$[A]$ of Eq. (37) for a pattern state.

6. Conclusions

In the present work, Rayleigh–Benard convection in a binary magnetic fluid liquid mixture under rotation is studied. We determine the stability thresholds for stationary convection for free-free boundary conditions. We found that, the binary effects drastically reduce the critical Rayleigh number and the magnetophoretic effect increases the critical

Rayleigh number. The weakly nonlinear analysis was performed and the analytical expression of the coefficient of the corresponding amplitude equation was obtained. Due to the binary and rotational effects a supercritical–subcritical transition appears. Also, the parameters regions for the Eckhaus instability and zigzag instability were found.

Acknowledgments

We would like to thank to Ms. K. Posso and Professor Clerc for their critical reading and their invaluable comments. This research received financial support from Anillo ACT 15 and ACT 24 of Bicentennial Program of Sciences and Technology-Chile, Millennium Science Nucleus P06-022-F, Convenio de desempeño UTA MECESUP-2 and FODECYT 11080229. L. M. Pérez acknowledges the USACH PhD program fellowship. Some of the numerical simulations was performed thanks to the simulation software DimX, developed at INLN.

References

Auernhammer, G. K. & Brand, H. R. [2000] "Thermal convection in a rotating layer of a magnetic fluid," *Eur. Phys. J. B* **16**, 157–168.

Berkovsky, B. M., Medvdev, V. F. & Krakov, M. S. [1973] *The Magnetic Fluids, Engineering Application* (Oxford University Press, Oxford).

Clerc, M. G., Escaff, D. & Rojas, R. [2008] "Transversal interface dynamics of a front connecting a stripe pattern to a uniform state," *Europhys. Lett.* **83**, 28002.

Finlayson, B. A. [1970] "Convective instability of ferromagnetic fluids," *J. Fluid Mech.* **40**, 753–767.

Gupta, M. D. & Gupta, A. S. [1979] "Convective instability of a layer of a ferromagnetic fluid rotating about a vertical axis," *Int. J. Eng. Sci.* **17**, 271–277.

Kaloni, P. N. & Lou, J. X. [2004] "Weakly nonlinear instability of a ferromagnetic fluid rotating about a vertical axis," *J. Mag. Mag. Mat.* **284**, 54–68.

Laroze, D., Martinez-Mardones, J., Bragard, J. & Vargas, P. [2006] "Convection in a rotating binary ferrofluid," *Physica A* **371**, 46–49.

Neuringer, J. L. & Rosensweig, R. E. [1964] "Ferrohydrodynamics," *Phys. Fluids* **7**, 1927–1937.

Newell, A. C. & Whitehead, J. A. [1969] "Finite bandwidth, finite amplitude convection," *J. Fluid Mech.* **38**, 279–303.

Ryskin, A. & Pleiner, H. [2004] "Influence of a magnetic field on the Soret-effect-dominated thermal convection in ferrofluids," *Phys. Rev. E* **69**, 046301.

Segel, L. A. [1969] "Distant side-walls cause slow amplitude modulation of cellular convection," *J. Fluid Mech.* **38**, 203–224.

Tagare, S. G., Benerji Babu, A. & Rameshwar, Y. [2008] "Rayleigh–Benard convection in rotating fluids," *Int. J. Heat Mass Transf.* **51**, 1168–1178.

Venkatasubramanian, S. & Kaloni, P. N. [1994] "Effects of rotation on the thermoconvective instability of a horizontal layer of ferrofluids," *Int. J. Eng. Sci.* **32**, 237–256.